EFFECT OF MATERIAL AND MANUFACTURING VARIATIONS
ON MEMBRANE ELECTRODE ASSEMBLY PRESSURE DISTRIBUTION

Andreas Vlahinos[1], Kenneth Kelly[2], Jim D'Aleo[3], Jim Stathopoulos[4],

[1]Advanced Engineering Solutions, LLC, Castle Rock, CO 80108, USA andreas@aes.nu
[2]National Renewable Energy Laboratory, Golden, CO 80401, USA kenneth_kelly@nrel.gov
[3]Plug Power, Inc., Latham, NY 12110, USA, james_daleo@plugpower.com
[4]Plug Power, Inc., Latham, NY 12110, USA jim_stathopoulos@plugpower.com

Abstract

A design is robust when it is not sensitive to variations in noise parameters such as manufacturing tolerances, material properties, environmental temperature, humidity, etc. In recent years several robust design concepts have been introduced in an effort to obtain optimum designs and minimize the variation in the product characteristics. Increasing the pressure on a PEM (Proton Exchange Membrane) fuel cell's MEA (Membrane Electrode Assembly) leads to increasing the electric conductivity and reducing the permeability of the assembly. In this study, a probabilistic FEA analysis was performed on a simplified fuel cell stack in order to identify the effect of material and manufacturing variations on the MEA's pressure distribution. The bi-polar flow plate thickness, the modulus of elasticity and the end plate bolt loading were considered as randomly varying parameters with given mean and standard deviation. The normal stress uniformity of the MEA was determined in terms of the probabilistic input variables. The methodology for implementing robust design used in this research effort is summarized in a reusable workflow diagram.

Introduction

The need for innovative tools is apparent now more than ever as more complex design requirements are surfacing such as cost, performance, safety, quality, time to market, short life cycle, environmental impacts, WOW aesthetics and major changes in industries' business models. Moreover, in new or emerging industries such the fuel cell industry the development time from concept to production is being compressed significantly. Furthermore robust fuel

cell designs are necessary in order for the to successfully compete with mature technologies.

Most organizations address the quality issue by focusing on implementation of Six Sigma in their manufacturing environments. Most of the manufacturing cost over the life cycle of a product is determined by its initial design, therefore quality issues must be addressed early in the design cycle with robust design methodologies.

The goal of robust design is to deliver customer expectations at affordable cost regardless of customer usage, degradation over product life and variation in manufacturing, suppliers, distribution, delivery and installation. Since randomness and scatter are a part of reality everywhere, probabilistic design techniques are necessary to engineer quality into designs. Traditional deterministic approaches account for uncertainties through the use of empirical safety factors. The safety factors are derived based on past experience [Ref 5]; they do not guarantee satisfactory performance and do not provide sufficient information to achieve optimal use of available resources. The probabilistic design process has not been widely used because it has been intimidating and tedious due to its complexity. In recent years, CAD and FEA codes have introduced integrated design space exploration (PTC's Behavioral Modeling [Ref 14]) and probabilistic systems (e.g. ANSYS' PDS [Ref 1, 3, 5 and 7]) that make probabilistic analysis simple to setup if the control and the noise parameters are identifiable [Ref 1]. Control parameters are those factors which the designer can control, such as geometric design variables, material selection, design configurations and manufacturing process settings, etc. [Ref 8]. Noise parameters on the other hand are factors
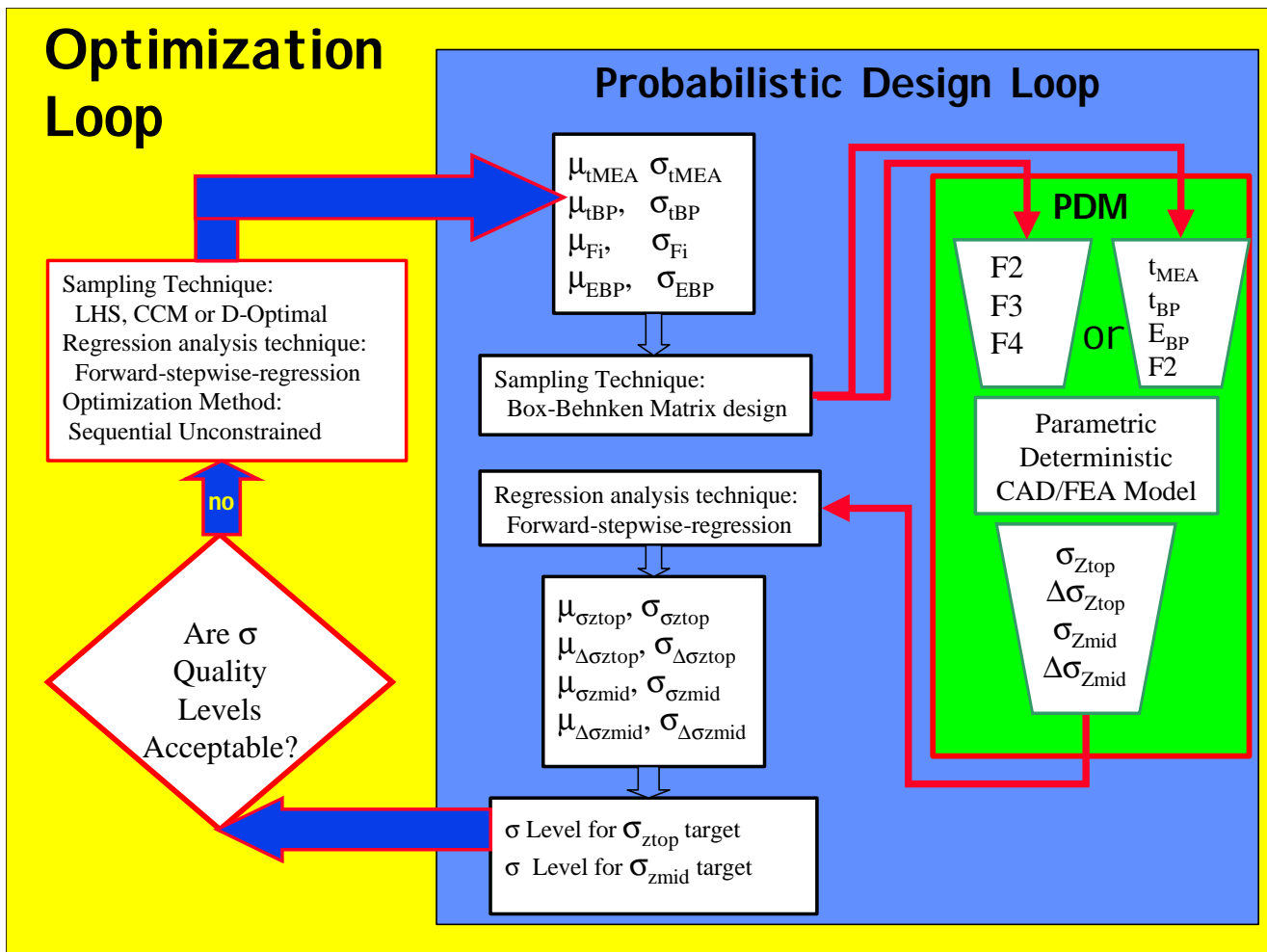
Optimization Loop

Probabilistic Design Loop

μ_{tMEA} σ_{tMEA}
$\mu_{tBP},$ σ_{tBP}
$\mu_{Fi},$ σ_{Fi}
$\mu_{EBP},$ σ_{EBP}

PDM

F2
F3
F4

or

t_{MEA}
t_{BP}
E_{BP}
F2

Sampling Technique:
  LHS, CCM or D-Optimal
Regression analysis technique:
  Forward-stepwise-regression
Optimization Method:
  Sequential Unconstrained

Sampling Technique:
  Box-Behnken Matrix design

Parametric
Deterministic
CAD/FEA Model

Regression analysis technique:
  Forward-stepwise-regression

σ_{Ztop}
$\Delta\sigma_{Ztop}$
σ_{Zmid}
$\Delta\sigma_{Zmid}$

no

$\mu_{\sigma ztop},\ \sigma_{\sigma ztop}$
$\mu_{\Delta\sigma ztop},\ \sigma_{\Delta\sigma ztop}$
$\mu_{\sigma zmid},\ \sigma_{\sigma zmid}$
$\mu_{\Delta\sigma zmid},\ \sigma_{\Delta\sigma zmid}$

Are σ
Quality
Levels
Acceptable?

σ Level for σ_{ztop} target
σ Level for σ_{zmid} target

Figure 1 Workflow for Robust Optimization

that affect the design's function and are beyond the control of the designer or too expensive to control or change.

Examples of noise parameters are material property variability, manufacturing process limitations, environmental temperatures, humidity, component degradation with time etc.

One of the keys to finding optimal and robust designs is exploring the nature of the design space. The goal is to identify the key design parameters that have the most impact on the product attributes. This paper describes a design for six-sigma technique that integrates FEA, probabilistic and robust design tools within the CAD environment. An example of a simplified fuel cell stack is used and the effect of material and manufacturing variations on the MEA's pressure distribution is identified.

Robust Design Process

The robust design process shown in Figure 1 has been implemented to evaluate the effect of bolt stack loading on the MEA pressure distribution. All of the symbols and processes will be described in subsequent sections. The effect of variation in the material properties such as the modulus of elasticity of the bi-polar plates E_{bp}, the bi-polar plate thickness t_{bp}, the MEA thickness t_{mea} and the bolt loading F have been also assessed.

This robust optimization workflow includes three different processes: the parametric deterministic model (PDM), the probabilistic design loop, and the design optimization loop.

The Parametric The Deterministic Model

A parametric finite element model of a simplified fuel cell stack assembly has been developed for the PDM process. Figure 2 shows the finite element model of the MEA and bi-polar plates assembly that contains twenty cells. The elements are color-coded based on their material properties. The material behavior was assumed to be linear elastic. The modules of elasticity and Poisson's ratios of the membrane, the bi-polar plate and the end plate are shown in table 1. The spacing of the flow and cooling channels, and

the thickness of the membrane and bi-polar plates are fully parametric. The dimensions shown are presented for demonstration purposes only; they don't necessarily reflect the actual hardware dimensions. A pair of aluminum end plates has been added on either side of the stack. Four bolts hold the stack together by imposing a 640 N force on each of the four corners of the end plates. Since the bolt load was applied at 8 nodes the nodal force considered was F = 80 N. Figure 9 shows the loading vectors applied at the end plate model. Under this loading condition the finite element model can easily predict the displacement and stress distribution on every component of the model. The first membrane's (closest to the end plate) maximum and minimum compression stress $\min\sigma_{ztop}$ and $\max\sigma_{ztop}$ can be easily found. The difference between maximum and minimum compression stress can be defined as the differential compression stress in the first membrane $\Delta\sigma_{ztop}$. The same set of values of stresses can be extracted from the membrane in the middle of the stack, specifically the maximum compression stress $\max\sigma_{zmid}$, the minimum compression stress $\min\sigma_{zmid}$ and the differential compression stress $\Delta\sigma_{zmid}$.
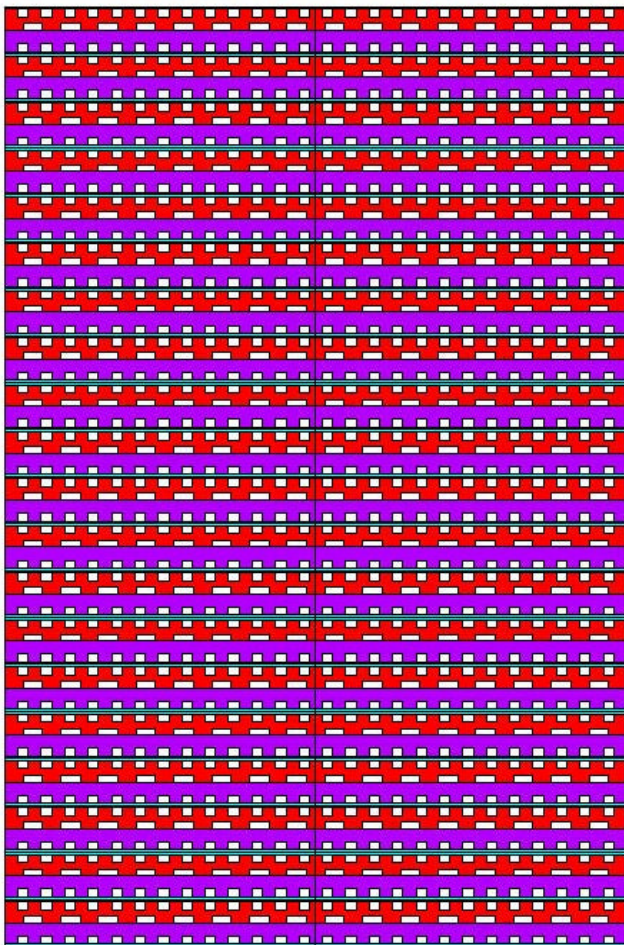
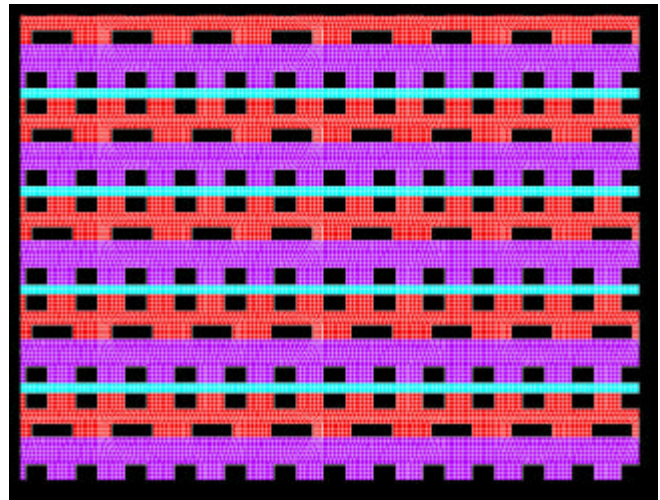Figure 2. Finite Element Model of the MEA and Bi-Polar Plates Assembly

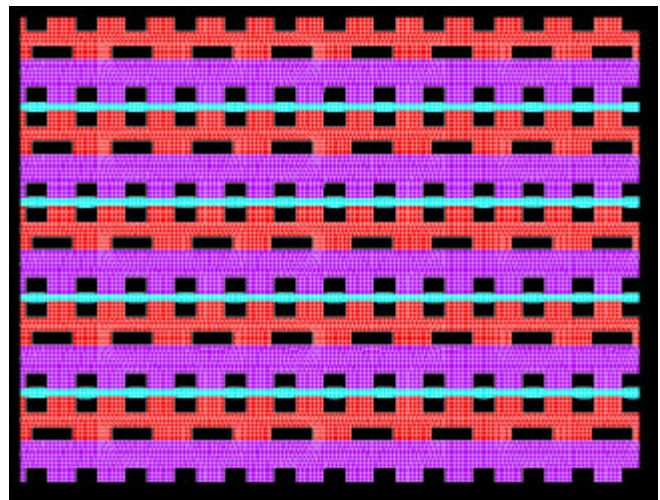Figure 3 Undeformed Shape of a Portion of the Model

Figure 4 Deformed Shape of a Portion of the Model

Figure 3 shows the un-deformed shape of a close up portion of the model. Figure 4 shows the deformed shape of the same region with unit displacement scale. One may observe that the membrane deformations are much larger than the bi-polar plate' deformations.

Table 1. Material Properties

	E (MPa)	ν
Membrane	21	0.001
Bi-polar Plates	5100	0.300
End Plate	70000	0.300

Figure 5 shows the Von Mises stress distribution and Figure 6 shows the compressive stress distribution of the same portion of the model. Since the compressive stress is negative the red portion of the distribution corresponds to zero stress level and the blue portion of the distribution corresponds to high negative values.
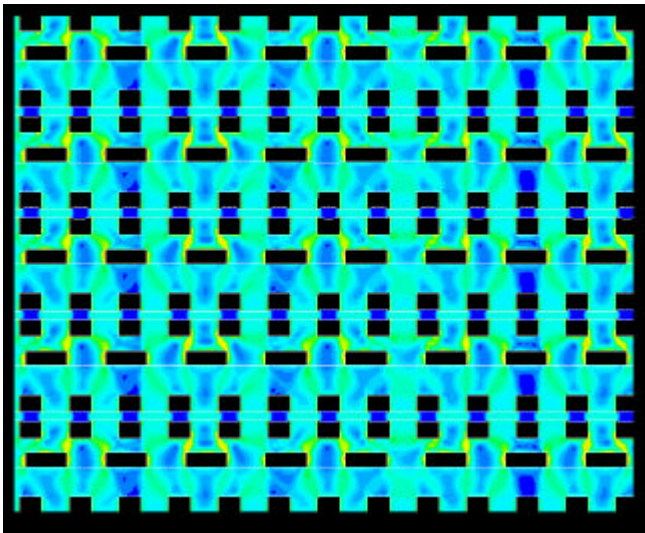
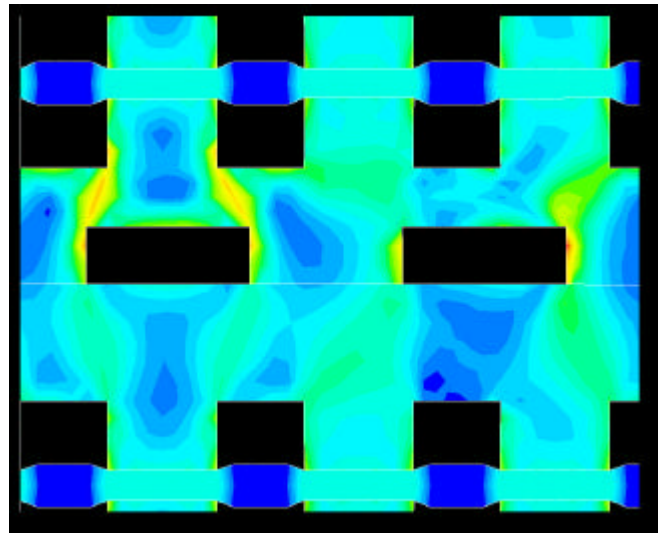Figure 5 Von Mises stress distribution of a portion of the model

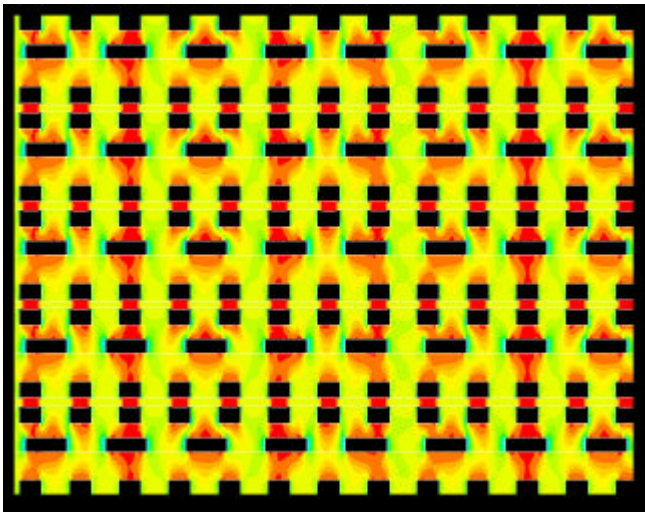Figure 7 Von Mises stress distribution of a small portion of the model

Figure 6 Compressive Stress σ_z Distribution of a Portion of the Model

Figure 8 Principal Stress Vectors on a small portion of the model

In Figure 6 one may observe the "load paths" (yellow flow streams) that carry the end plate loading from one side to another. Figure 7 shows the Von Mises stress distribution of a small portion of the model and Figure 8 shows a plot of the principal stress vectors on a small portion of the model.

Effect of Bolt Load Variation on the MEA'S pressure uniformity

Due variations in the assembly process the magnitude of the bolt forces may exhibit variation. For this analysis all geometric parameters, material properties and the first bolt load were held constant at F1 = 8*80 N (F1 = 640 N).
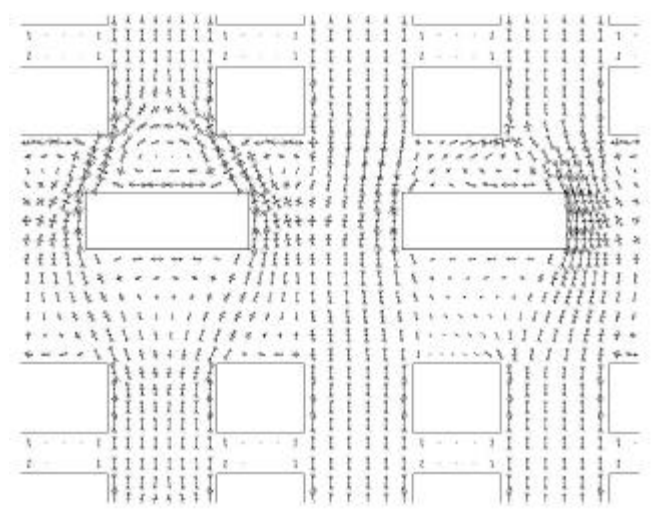
The other three bolt loads F2, F3 and F4 exhibit variation with normal distribution of mean values:

$$\mu_{F2} = \mu_{F3} = \mu_{F4} = 8*80 \text{ N}$$

and standard deviations:

$$\sigma_{F2} = \sigma_{F3} = \sigma_{F4} = 8*4 \text{ N}$$

The random values of the three bolt loads are independent of each other. Figure 10 shows the probability density functions of the three bolt loads F2, F3 and F4. In this study all other geometric and material parameters remain constant in the three-dimensional finite element model.
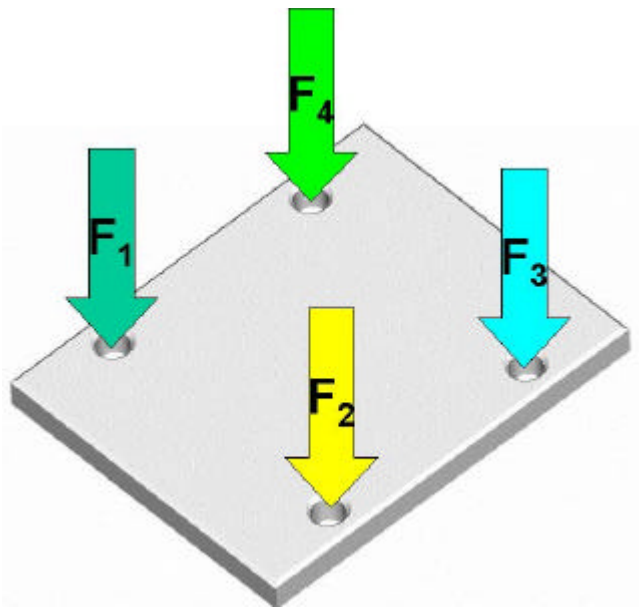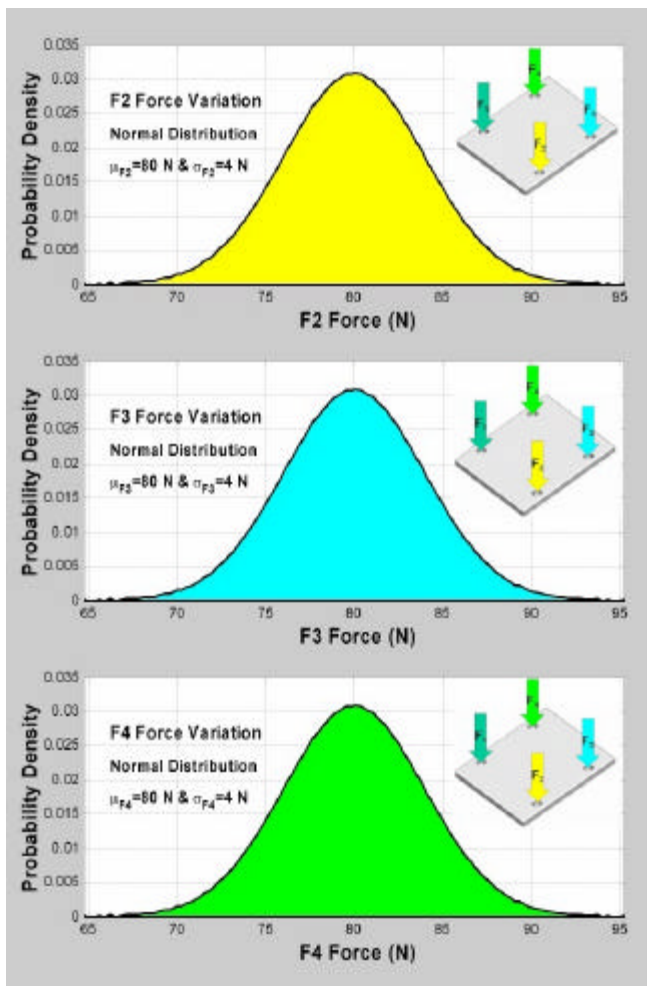
Figure 9 Loading Vectors at the Endplate
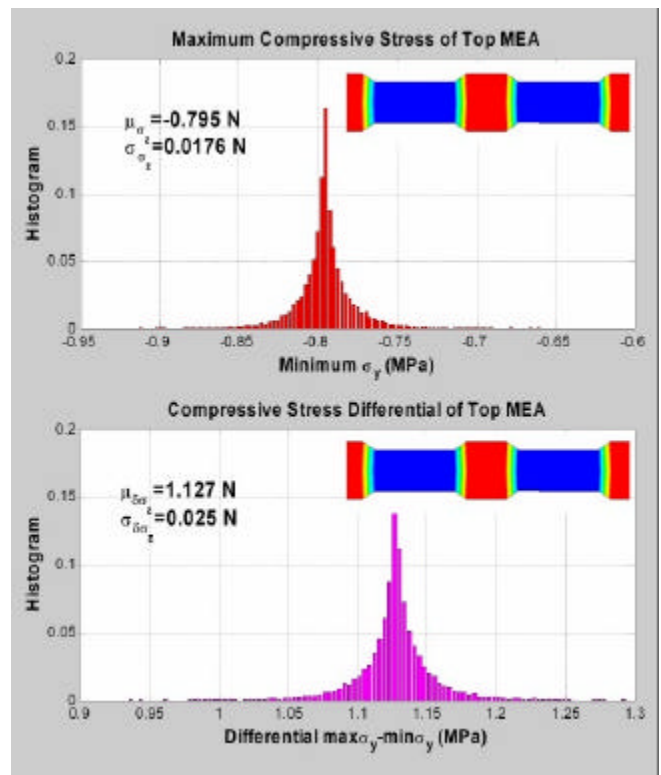

Figure 11 Histograms of maximum maxσ_{ztop} and differential compressive stress $\Delta\sigma_{ztop}$ in the top MEA

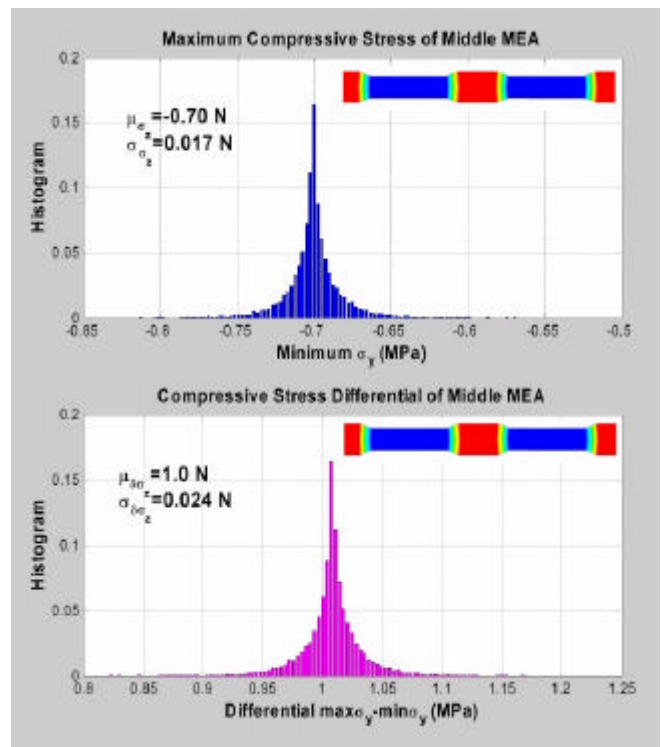Figure 10 Probability Density Functions of the three bolt loads F2, F3 and F4

Figure 12 Histograms of maximum maxσ_{zmid} and differential compressive stress $\Delta\sigma_{zmid}$ in the middle MEA

For a given set of the mean values of these bolt loads (input design variables) and the assumed distributions one may easily generate a large set of random numbers for each variable. Several sampling techniques are available to generate combination sets of these design variables such as Monte Carlo, Latin Hypercube Sampling (LHS), Central Composite, Box-Behnken Matrix, etc. If the "experiment" is fast and inexpensive Monte Carlo and LHS sampling techniques work well. In this case the "experiment" is a structural finite element analysis. If the "experiment" is time consuming and computationally expensive Box-Behnken Matrix in combination with the response surface technique is preferred. In this example Box-Behnken Matrix sampling was used in combination with Forward-stepwise-regression.

The probabilistic design loop is fully automated. If one views this loop as a transfer function the mean values and standard deviations of the three design variables (bolt loads) can be considered as inputs (μ_{F2}, μ_{F3}, μ_{F4}, σ_{F2}, σ_{F3}, σ_{F4}) and the mean and standard deviation of the attributes (maximum σ_z and differential compressive stress $\Delta\sigma_z$ in the top and middle MEAs) can be considered as outputs ($\mu_{\sigma ztop}$, $\sigma_{\sigma ztop}$, $\mu_{\Delta\sigma ztop}$, $\sigma_{\sigma\Delta ztop}$, $\mu_{\sigma zmid}$, $\sigma_{\sigma zmid}$, $\mu_{\Delta\sigma zmid}$, $\sigma_{\Delta\sigma zmid}$). Figure 1 shows a graphical representation of the data flow for this loop.

Execution of the probabilistic design loop will result in a probabilistic distribution of the response attributes. The mean value and standard deviation of the maximum compressive stress σ_z in the top MEA are $\mu_{\sigma ztop} = -0.795$ MPa and $\sigma_{\sigma ztop} = 0.0176$ MPa. The mean value and standard deviation of the differential compressive stress $\Delta\sigma_z$ in the top MEA are $\mu_{\Delta\sigma ztop} = 1.127$ MPa and $\sigma_{\sigma\Delta ztop} = 0.025$ MPa. Figure 11 shows the histograms of maximum $max\sigma_{ztop}$ and differential compressive stress $\Delta\sigma_{ztop}$ in the top MEA. Using these values one can quantify the quality of the design and determine the sigma level by solving for "n" in the following equation.

$$\mu_{\Delta\sigma top} - n * \sigma_{\Delta\sigma top} \leq \Delta\sigma_{Target} \qquad Eq(1)$$

where σ_{Target} is the target or maximum allowable differential compressive stress $\Delta\sigma_z$.

The mean value and standard deviation of the maximum compressive stress σ_z in the middle MEA are $\mu_{\sigma ztop} = -0.70$ MPa and $\sigma_{\sigma ztop} = 0.0176$ MPa. The mean value and standard deviation of the differential compressive stress $\Delta\sigma_z$ in the top MEA are $\mu_{\Delta\sigma top} = 1.00$ MPa and $\sigma_{\Delta\sigma top} = 0.024$ MPa. Figure 12 shows the histograms of maximum $max\sigma_{ztop}$ and differential compressive stress $\Delta\sigma_{ztop}$ in the middle MEA. The numerical results are summarized in Table 2.
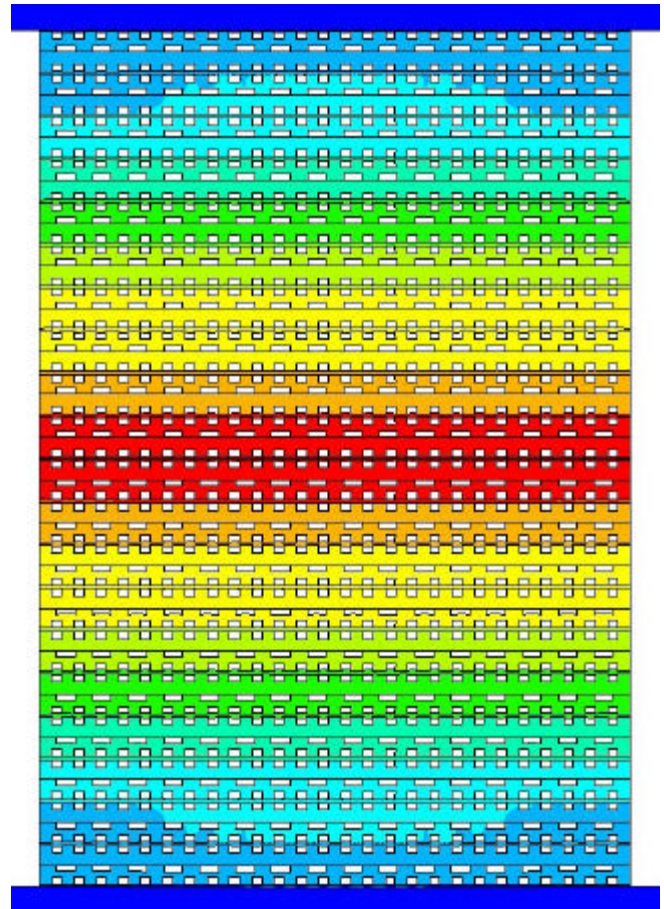

Figure 13 Displacement Distribution at mean values of the design variables

The top MEAs' maximum compressive stress $max\sigma_z$ and differential compressive stress $\Delta\sigma_z$ are about 13% higher that the equivalent values of the middle MEA. Only the first few MEAs at the top and bottom of the stack experience the higher stress level "edge effect" as shown in Figure 13. The compliance of the "soft goods" of the first few cells provides uniformity in pressure distribution at the majority of the MEAs.

Table 2. Effect of Bolt Load Variation on the MEA'S pressure uniformity

MEA	Stress	Mean Value μ (MPa)	Standard Deviation σ (MPa)
Top	$max\ \sigma_z$	-0.795	0.0176
	$max\ \Delta\sigma_z$	1.127	0.025
Middle	$max\ \sigma_z$	-0.700	0.017
	$max\ \Delta\sigma_z$	1.000	0.024

Effect of Bolt Load, Material and Thickness Variation on the MEA'S pressure uniformity

In this case study four input design variables were considered having variation, the MEA thickness t_{MEA}, the bipolar plate thickness t_{BP}, the modulus of elasticity of the bipolar plates and the bolt load of two of the bolts F2.

It was assumed that the 1st and 4th bolt loads remain constant at F1 = F4 = 100 N. The other two bolt loads, F2 and F3, exhibit variation with normal distribution of mean values:

$$\mu_{F2} = \mu_{F3} = 100 \text{ N}$$

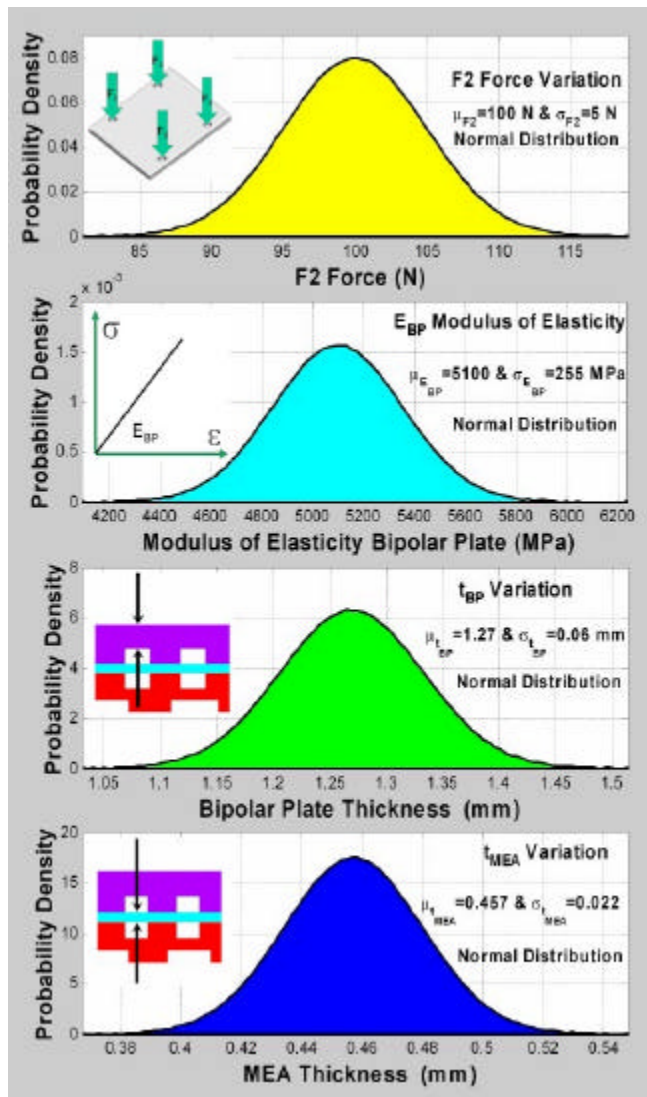and standard deviations:

$$\sigma_{F2} = \sigma_{F3} = 5 \text{ N}$$

Figure 14 Probability Density Functions of case 2 Design Variables F2, F3, E_{BP}, t_{BP} and t_{MEA}

The random values of the two bolt loads are dependent. Figure 14a shows the probability density functions of the two bolt loads, F2 and F3. The modulus of elasticity of the bipolar plates E_{BP} exhibits variation with normal distribution and mean value μ_{EBP} = 5100 MPa and standard deviation σ_{EBP} = 255 MPa. Figure 14b shows the probability density functions of the modulus of elasticity variation.

The bipolar plate thickness t_{BP} exhibits variation with normal distribution and mean value μ_{tBP} = 1.27 mm and standard deviation σ_{tBP} = 0.06 mm. Figure 14c shows the probability density functions of the bipolar plate thickness variation. The MEA thickness t_{MEA} exhibits variation with normal distribution and mean value μ_{tMEA} = 0.457 mm and standard deviation σ_{tMEA} = 0.022 mm. Figure 14d shows the probability density functions of the MEA thickness variation.

Table 3. Effect of Bolt Load, Modulus of Elasticity, Bipolar Plate and MEA thickness Variation on the MEA'S pressure uniformity

MEA Loc.	Max Stress	Mean Value μ (MPa)	Standard Deviation σ (MPa)	Skewness Coeff.
Top	σ_z	-7.34	2.081	-1.705
	$\Delta\sigma_z$	6.388	2.104	1.822
Middle	σ_z	-5.58	0.403	-2.760
	$\Delta\sigma_z$	5.846	0.434	2.654

Execution of the probabilistic design loop for these load combinations will result in a probabilistic distribution of the response attributes. A summary of the results is presented in table 3. The mean value and standard deviation of the maximum compressive stress σ_z in the top MEA are $\mu_{\sigma ztop}$ = -7.34 MPa and $\sigma_{\sigma ztop}$ = 2.081 MPa. The mean value and standard deviation of the maximum compressive stress σ_z in the middle MEA are $\mu_{\sigma zmid}$ = -5.58 MPa and $\sigma_{\sigma zmid}$ = .0403 MPa. Figure 15 shows the histograms of the maximum compressive stresses on the top and middle MEAs $\max\sigma_{ztop}$ and $\max\sigma_{zmid}$. Although all input parameters exhibit variation with normal distributions the output parameters exhibit a high degree of asymmetry of their distribution around their mean. The skewness coefficient characterizes the degree of asymmetry of these distributions and is shown in table 3. Both compressive stress $\max\sigma_z$ distributions have negative skewness, that indicates distributions with an asymmetric tail extending towards more negative values as shown in figure 15. Both differential stress $\max\Delta\sigma_z$ distributions have positive skewness, that indicates a

distribution with an asymmetric tail extending towards more positive values as shown in figure16.

The mean value of the compressive stress of the top of the MEAs is significantly higher (30%) than the corresponding value of the middle MEA. In addition the standard deviation of the top MEA is 5 times larger than the middle MEA indicating a large scatter of values. In other words the manufacturing, material and loading imperfections have great effect on the stress values of the top MEA. This conclusion can also be made for the first few MEAs on the top and bottom of the fuel cell stack. Due to the compliance of the "soft goods" the majority of the MEAs appear to be insensitive to the manufacturing variations within the range considered in this research effort. Figure 17 shows a bar chart of the value of the maximum differential compressive stress in all the MEAs of the model. In this case the "edge effect" is extended to the top four MEAs and their value monotonically decreases as we move from the endplate to the center of the stack.

Figure 16 shows the histograms of the maximum differential compressive stresses on the top and middle MEAs. Similar conclusions can be made for the differential compressive stress of the top and bottom MEAs.

The probabilistic loop can generate a large number of data points using the response surface function. In this case 10,000 points were generated to examine the effect of manufacturing variations. Using this data it's relatively easy to extract the sensitivity of the input variables to the output variables. Figure 18 shows the sensitivity of all the design variables on pressure uniformity of the top and middle membranes. The bipolar plate thickness and the MEA thickness are the most significant factors on the top membranes' pressure uniformity as shown in figure 17. The bolt force and modules of elasticity of the bipolar plates are insignificant factors on the top membranes' pressure uniformity. The bolt force, the MEA thickness and the modules of elasticity of the bipolar plates are the most influential input variables on the pressure uniformity of the MEAs in the middle of the stack.
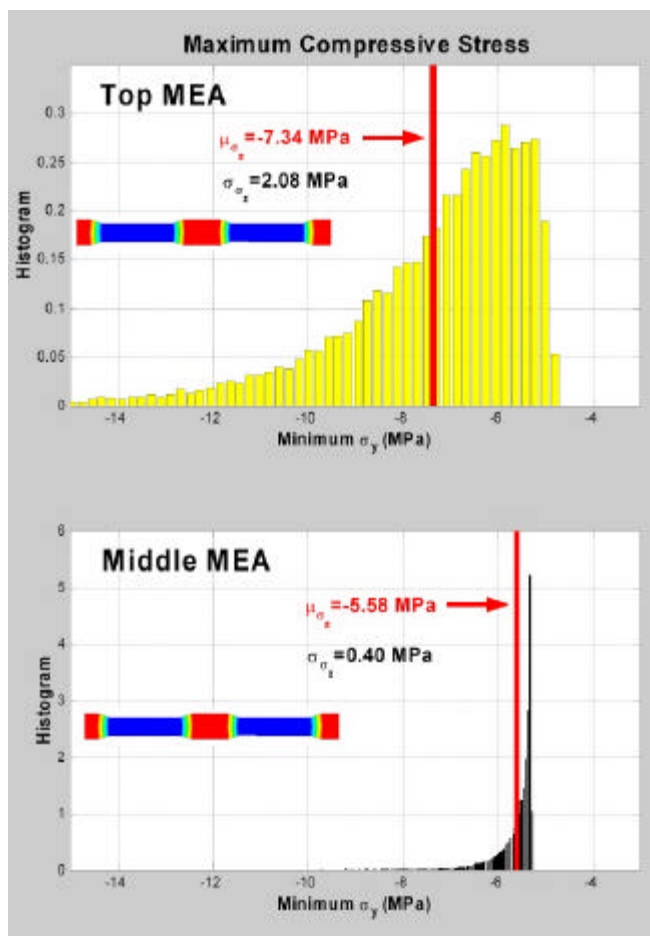

Figure 15 Histograms of maximum compressive stress in the top and middle MEA
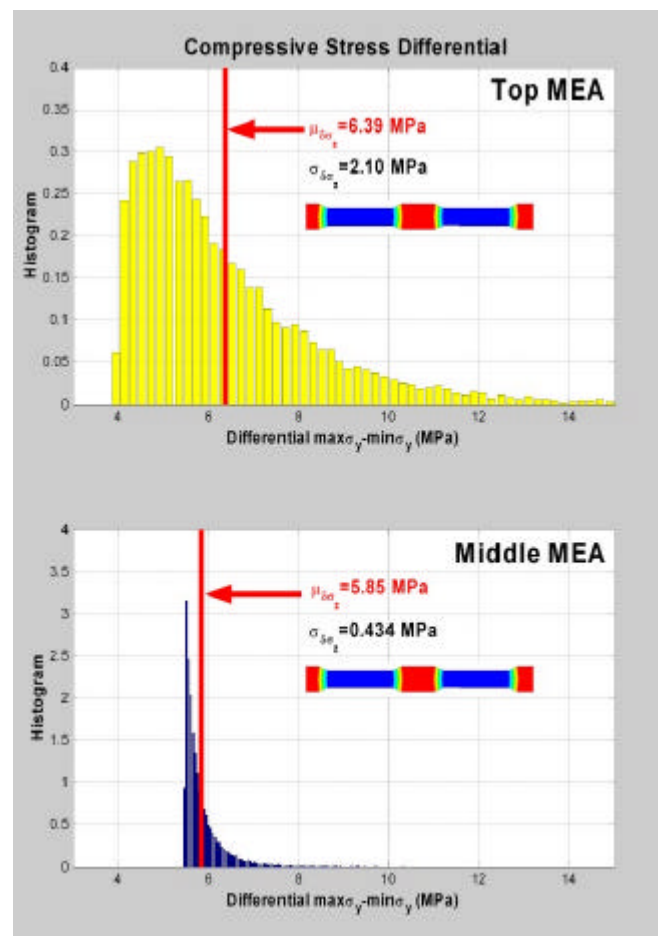

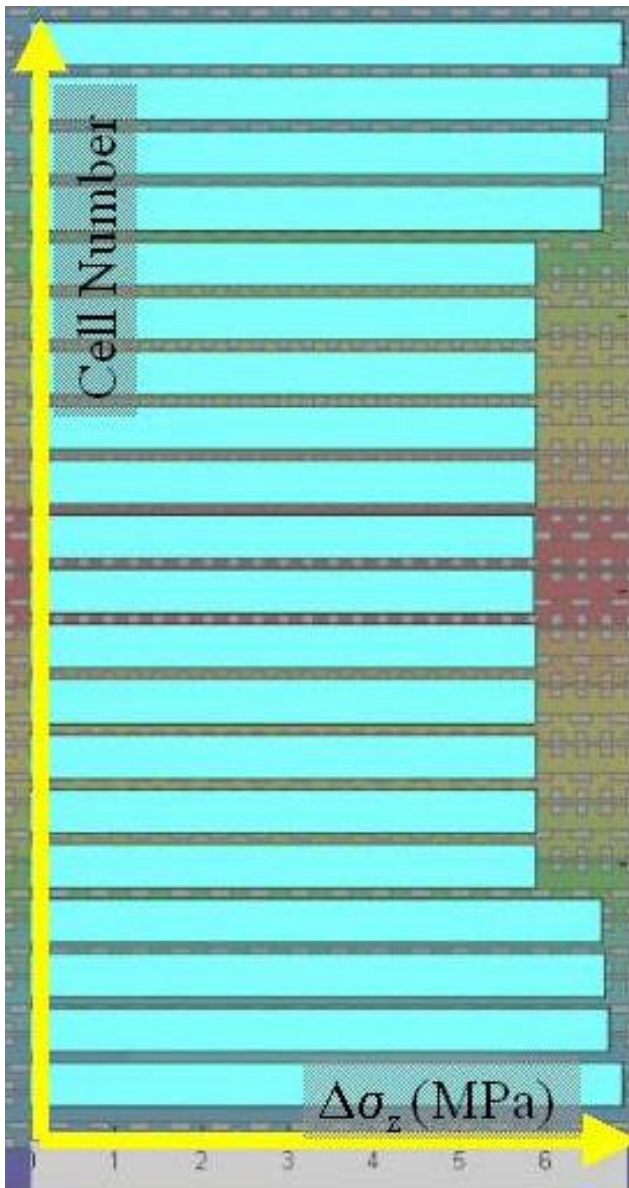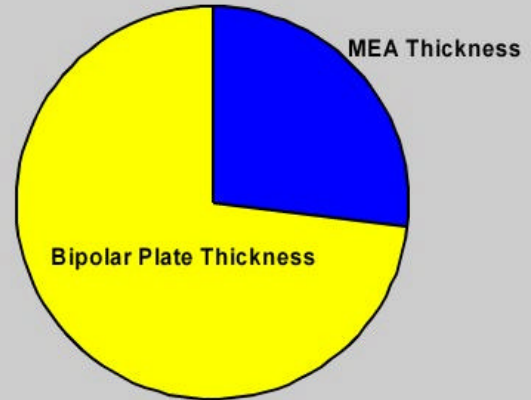Figure 16 Histograms of maximum differential compressive stress in the top and middle MEA

Figure 17 Bar chart of differential compressive stress in all the MEAs

Figure 18 Sensitivity of Design Variables on Pressure Uniformity

Conclusions

For the set of design variables and their range examined the following conclusions can be made:

- In the bolt load variation case the top MEAs' maximum compressive stress $\max\sigma_z$ and differential compressive stress $\Delta\sigma_z$ are about 13% higher that the equivalent values of the middle MEA.

- For the case where all design variables have variation the mean value of the compressive stress of the top of the MEAs is significantly higher (30%) than the corresponding value of the middle MEA.

- Only the first few MEAs at the top and bottom of the stack experience the higher stress level "edge effect." The compliance of the "soft goods" of the first few cells provides uniformity in pressure distribution at the majority of the MEAs.

- The bolt force, the MEA thickness and the modules of elasticity of the bipolar plates are the most influential input variables on the pressure uniformity of the MEAs in the middle of the stack.

- The probabilistic analysis described allows engineers to gain greater insight into complex engineering processes that involve statistical variations and enables them to identify better designs that meet the performance objectives and are less sensitive to manufacturing variations.

Acknowledgments

References

1. ANSYS Inc. <u>Probabilistic Design Techniques</u>, Advanced Analysis Techniques Guide, August 2002

2. Breyfogle, F., Cupello, J., Meadows, B., <u>Managing Six Sigma: a practical guide to understanding, assessing, and implementing the strategy that yields bottom-line success,</u> John Wiley, New York 2001.

3. Chen X., Hasselman T.K, and Neill D.J., "Reliability Based Structural Design Optimization for Practical Applications," 38th AIAA/ASME/ASCE/AHS/ASC, Structures, Structural Dynamics and Materials Conference, paper # AIAA-97-1403, Kissimmee, FL 1997

4. Creveling, C., Slutsky, J., Antis, D., <u>Design for Six Sigma : in technology & product development</u> Prentice Hall Upper Saddle River, NJ, 2003

5. Haldar A. and Mahadevan S., <u>Reliability Assessment Using Stochastic Finite Element Analysis</u>, John Wiley, 2000, New York, New York.

6. Harry, M. and Schroeder, R. <u>Six sigma: the breakthrough management strategy revolutionizing the world's top corporations</u>, Doubleday, New York 2000.

7. Marckzyk J., <u>Principals of Simulation-based Computer-aided Engineering</u>, FIM Publications, September 1999

8. Pande, P., Neuman, R, Cavanagh, R, <u>The Six Sigma way : how GE, Motorola, and other top companies are honing their performance</u> McGraw-Hill, New York , 2000

9. Phadke M. S., <u>Quality Engineering Using Robust Design</u>, Prentice Hall, 1989.

10. Schmidt, R. and Launsby S., <u>Understanding Industrial Designed Experiments</u>, 4th edition, Air Academy Press, 2000.

11. Vanderplaats Research and Development, Inc. <u>VisualDOC Design Optimization Software</u>, Version 3.0, August 2002

12. Vlahinos A. and Kelkar S. "Body-in-White Weight Reduction via Probabilistic Modeling of Manufacturing Variations," *2001 International Body Engineering Conference*, SAE paper # 2001-01-3044, Detroit, MI, October 2001

13. Vlahinos A. and Kelkar S. "Designing For Six-Sigma Quality with Robust Optimization using CAE," *2002 International Body Engineering Conference*, SAE paper # 2002-01-2017, Paris, France, July 2002

14. Vlahinos, A. <u>Engineering Quality into Designs Using Behavioral Modeling</u>, Training Manual, 2002 PTC/USER World Event, Atlanta, GA, June 2002

15. Vlahinos, A., Penney T. and Kelkar S. " Engineering Quality into Digital Functional Vehicles," proceedings of IDPS2002, *2002 Daratech Intelligent Digital Prototyping Strategies Conference*, Detroit, MI, June 2002

16. Vlahinos A., Kelly K., Pesaran A., Penney T., "Empowering Engineers to Generate Six-Sigma Quality Designs" Proceedings of *First Annual Quality Paper Symposium, American Society for Quality, Automotive Division*, Livonia, MI, February 2003.